

# Acoustic Sediment Classification Using High-Frequency (400 kHz) Multibeam Data in Pari Water of Seribu Island, Indonesia

Dadang Handoko<sup>1</sup>, Henry M. Manik<sup>2\*</sup>, Totok Hestirianto<sup>2</sup>, Karlisa Priandana<sup>3</sup>,  
Rozaimi Che Hasan<sup>4</sup>

<sup>1</sup>Marine Technology Study Program, Department of Marine Science and Technology,  
Faculty of Fisheries and Marine Sciences, IPB University

<sup>2</sup>Department of Marine Science and Technology, Faculty of Fisheries and Marine Science, IPB University

<sup>3</sup>Department of Computer Science, School of Data Sciences and Informatics IPB University  
Jl. Raya Darmaga Kampus IPB, Bogor, Jawa Barat 16680, Indonesia

<sup>4</sup>Department of Generative AI, Faculty of Artificial Intelligence, Universiti Teknologi Malaysia  
Jalan Sultan Yahya Petra (Jalan Semarak) 54100 Kuala Lumpur, Malaysia  
Email: henrymanik@apps.ipb.ac.id

## Abstract

Seafloor classification is essential for understanding sediment distribution, marine habitat characteristics, and resource management. Therefore, this study aimed to classify seafloor sediment in the Pari water, Indonesia using high-frequency (400 kHz) backscatter data obtained through the Multibeam Echosounder T-50P. The Angular Range Analysis (ARA) method was applied to analyze backscatter intensity variations across different incidence angles, to enhance the accuracy of sediment classification in this shallow marine environment. Data acquisition was collected using the T-50P, which captured high-resolution acoustic signals from varying angles to generate angular response curves. Analysis was conducted in the curves were then analyzed to differentiate sediment types, with ground-truth sediment samples collected to validate classification outcomes. The result showed that backscatter intensity mosaic had an intensity range of -27 dB to -37.5 dB. Applying ARA enabled the identification of 12 sediment classes, including sandy silt, coarse silt, and clayey sand. Sediment distribution maps, generated via FMGT and visualized with ArcGIS, indicated a predominance of fine-grained sediments. The FMGT-based classification tended to prioritize finer sediment categories, likely due to the acoustic limitations in detecting granular details. Conversely, the in-situ analysis of 15 sediment samples revealed medium sand as the predominant sediment type, accompanied by smaller proportions of coarse sand and coral fragments. The discrepancies between the in-situ sampling and FMGT results were primarily due to the operational frequency of the MBES system, which limits the acoustic signal's penetration to the surface of the seabed. This highlights the importance of in-situ sampling to complement acoustic data, especially in accurately seabed characterization.

**Keywords:** Pari Island, Multibeam Echosounder System (MBES), Backscatter, Seafloor Classification

## Introduction

Multibeam Echosounder System (MBES) is a reliable tool for surveying and mapping underwater, by emitting high-frequency sound waves, MBES gathers detailed data on seafloor topography (bathymetry) and backscatter intensity, essential for seafloor classification (Innangi *et al.*, 2015). Acoustic methods to identify, classify, and map seafloor resources have significantly advanced the effectiveness of marine surveys and mapping (Manik, 2012). Acoustic techniques provide non-invasive, rapid, and cost-effective solutions compared to conventional methods, making them indispensable for modern seafloor mapping initiatives, especially in shallow coastal regions (Manik *et al.*, 2006). These acoustic responses vary with factors such as frequency (Frederick *et al.*, 2020) and seafloor composition, where different sediment types produce

distinct backscatter intensities (Manik *et al.*, 2015; Fahrulian *et al.*, 2016).

Two different backscatter formats from MBES are commonly used for sediment classification: backscatter mosaic and angular backscatter response. Backscatter mosaic is generally used with image-based analysis and classification and provides good visualization in terms of 2-Dimensional spatial resolution of the seabed reflectance (Janowski *et al.*, 2018). The latter (angular backscatter response) is also useful in differentiating sediment types in terms of backscatter intensities at different incidence angles.

Angular backscatter response has more characterization capability than backscatter mosaic as the range of incidence angles across MBES swath varies (typically from 0-65), thus providing

advantages in sediment classification. The use of angular backscatter response has been limited due to its low spatial resolution and 2D visualization. However, angular backscatter response has been demonstrated to be useful towards remote characterization of the sediment types such as the development of Angular Range Analysis (ARA) (Fonseca and Mayer, 2007). Although this method has been made commercially in many MBES processing software, there are limited studies that evaluate this method for sediment characterization, especially in Indonesia coastal waters using high frequency MBES.

Angular Range Analysis (ARA) has been employed as an advanced method for analyzing MBES data to enhance sediment classification accuracy. ARA examines variations in backscatter intensity across different incidence angles, making it possible to distinguish between fine and coarse sediments more accurately. Using high-frequency acoustic data, such as 400 kHz, allows for higher resolution and better differentiation of sediment types, particularly in shallow water environments, where precision is crucial.

This study focuses on Pari Island in the Seribu Islands, Indonesia, a shallow coastal region with complex sediment compositions and active marine ecosystems. The waters surrounding Pari Island in the Seribu Islands, Indonesia, represent a unique and complex coastal ecosystem with small islands of white sandy beaches and coral reefs, essentially a cluster of coral islands formed and shaped by coral biota and their associated organisms (algae, mollusks, foraminifera, and others) through natural dynamic processes (Mustikasari and Rustam, 2019).

Characterized by diverse sediment compositions, coral reefs, seagrass beds, and human activities, this region presents both opportunities and challenges for seafloor mapping and classification. Accurate sediment classification in this area is essential for environmental monitoring, coastal management, and habitat conservation. By applying ARA to high-frequency (400 kHz) MBES data, this study aims to produce a detailed classification of seafloor sediments in the Pari Island waters. The research outcomes are expected to improve understanding of sediment distribution in tropical shallow waters, supporting efforts in sustainable coastal management and providing insights for future acoustic classification studies in similar environments.

## Material and Methods

### Acoustic data acquisition

Field data acquisition was conducted on 27 June 2024. One of the results of a bathymetric survey using the Reson T-50P with frequency 400 kHz Multibeam Echosounder and the raw data used in this study with file format (\*.s7k). Inertial Motion Unit (IMU) sensor DMS 05 is used to measure the ship's attitude, including pitch, roll, and yaw parameters. Additionally, the ship's heading and horizontal positioning are determined using GNSS differential (Global Navigation Satellite System), ensuring accurate location tracking and movement corrections during the data collection process. The offset calibration in the Multibeam Echo Sounder (MBES) system is performed to correct errors caused by installation mistakes or shifts/distortions in the

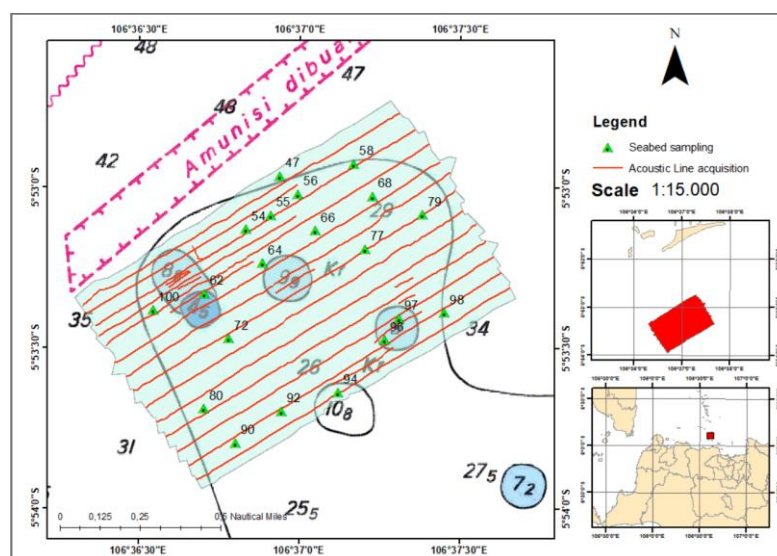


**Figure 1.** The acoustic survey track in the red line was located in Pari water and the sediment sample in the green triangle

transducer array. By determining the patch test values during the calibration of the Multibeam Echosounder (MBES) system, several errors were observed: a roll error of  $-1.18^\circ$ , a pitch error of  $-1.13^\circ$ , and a yaw error of  $-0.78^\circ$ . Additionally, the latency measured was 0.00 m/s. These observed errors indicate the need for adjustments to ensure accurate measurements during survey operations, the state of the vessel was refined using the raw data obtained from the MBES Reson T-50R bathymetric measurement system.

**Oceanographic parameter**

The seabed sediment sampling in the study area around Pari Island was conducted at 20 station points using a Van Veen grab, as shown in

Figure 1. Samples were then analyzed in a sediment laboratory to determine the sediment type at each station. The sound velocity profile data in seawater was collected through a Valeport turbidity sensor, which was useful for correcting acoustic data. The speed of sound in water was significantly influenced by chemical and physical parameters, as it changed with variations in temperature, salinity, pressure, and depth in a given body of water (Asmoro et al., 2024).

**Data analysis**

The acoustic data obtained from MBES represented the amplitude values of backscatter from the seafloor. The backscatter measurement principle used in the MBES Reson T50P is as follows (Wendelboe, 2018):

$$S_b = 10 \log 10(\sigma) \tag{1}$$

$$\sigma = \frac{\langle |P_s|^2 \rangle r^4}{P_0^2 r_0^2 B_{T_{xz}}^2 e^{(-4k''_w r)} A} \tag{2}$$

Where  $S_b$  is backscatter intensity,  $\sigma$  is scattering cross section,  $\langle |P_s|^2 \rangle$  is the mean square value of the backscattered sound pressure originating from a large number of small patches within an insonified area  $A$ , measured at the distance  $r$ . The transmit peak pressure at  $r_0 = 1$  m from the source is  $P_0$ ,  $B_{T_{xz}}$  is the normalized across-track beam pattern of the transmitter, and  $k''_w$  is the exponential coefficient for absorption in the water.

Reson T-50P multibeam echosounder (MBES), operating at a frequency of 400 kHz, was employed for high-resolution hydrographic data acquisition. The PDS2000 acquisition software was used to generate raw data that encompass bathymetric and backscatter information. In this study, data were wprocessed using the post-processing software Fledermaus Geocoder Toolbox (FMGT) (Fonseca et

al., 2002; Fonseca and Calder, 2005, 2007). Data extraction is transformed into georeferenced images based on a raster foundation. The stages of correcting the backscatter data from the seafloor include beam pattern correction, auto gain, time-varying gain, angle-varying gain, and anti-aliasing. These processes are essential for producing mosaics that yield accurate intensity values of the seafloor backscatter, as described by (MacDonald and Collins, 2008).

To obtain a backscatter mosaic, the process required requires two raw data formats from the MBES acquisition, namely \*.s7k and \*.gsf data. The \*.s7k data contained information on depth and backscatter intensity, while the Generic Sensor Format (.gsf) data provided bathymetric information, which supports mosaic processing. The seafloor backscatter mosaic was computed using radiometric and geometric corrections, with additional processing for mapping, noise reduction, and seam artifact removal to ensure a seamless and accurate result, which can be calculated using equation 3 by (Fonseca and Calder, 2005). Additionally, the equation was adopted from the mathematical model by (Jackson et al., 1986).

$$\sigma_r(\theta, f) = F(\theta, f; \rho, v, \delta, \omega_2, \lambda) \tag{3}$$

where  $\sigma_r$  is the interface backscattering cross-section per-unit solid angle per unit area,  $\theta$  is the grazing angle,  $f$  is frequency,  $\rho$  is the ratio of sediment mass density to water mass density,  $v$  is the ratio of sediment sound speed to water sound speed,  $\delta$  is the loss parameter: ratio of imaginary to real wave number for the sediment,  $\omega_2$  is the spectral strength of the bottom relief spectrum ( $\text{cm}^4$ ) at wave number  $1 \text{ cm}^{-1}$ , and  $\lambda$  is the spectral exponent of the bottom relief spectrum.

Data obtained includes salinity, depth, and temperature, which were will later be used to calculate the sound velocity profile at various depths (Nugroho et al., 2022) using a simple formula as follows: (Medwin, 1975; Medwin et al., 1998; Makar, 2022)

$$c(S, T, D) = 1449 + 4.6T - 0.055T^2 + 0.0003T^3 + (1.39 - 0.012T)(S - 35) + 0.016D \tag{4}$$

where  $c$  is the speed of sound ( $\text{m}\cdot\text{s}^{-1}$ ),  $T$  temperature ( $^\circ\text{C}$ ),  $S$  salinity (ppt) and  $D$  depth (meters).

Sediment processing involved drying the samples, followed by oven-drying until fully desiccated. After drying, each sample was weighed accurately. Dry sieving was conducted on sediment samples to determine the grain size distribution across the following size fractions:  $>4.75 \text{ mm}$ ,  $>2$

mm, 1 mm, 0.5 mm, 0.25 mm, 0.125 mm, 0.063 mm, and <0.063 mm. The procedure involved passing the sediment through a series of sieves with decreasing mesh sizes to separate and quantify each fraction by weight, providing a detailed granulometric profile of the sample. Subsequently, the samples were subjected to dry sieving using a sieve shaker for 15 minutes at a vibration amplitude of 3 to ensure uniform separation of sediment particles. This sieving process separated the sediment into distinct grain size fractions, allowing for detailed substrate classification based on particle size (Folk and Ward, 1957).

**Result and Discussion**

**Backscatter intensity**

The backscatter intensity value is relative due to the backscatter intensity calibration not performed on the Reson T-50P sonar head. The backscatter intensity mosaic derived from MBES data acquisition at a frequency of 400 kHz in the Pari Island water showed an intensity range from -27 dB to -37.5 dB. High backscatter intensities are represented by brighter tonal values, while lower intensities appear as darker tones, as illustrated in the accompanying Figure 2. Variability in backscatter intensity is attributed to factors such as the hardness, roughness, and porosity of the seabed sediment (Manik, 2015). Based on Figure 5, the processing of the backscatter mosaic was conducted using FMGT software. The resultant mosaic featured varying shades of gray, which corresponded to different levels of backscatter intensity captured by the Multibeam Echo Sounder (MBES) system. However, the mosaic values of backscatter intensity were not a strong parameter for representing the acoustic response of the seafloor (Fonseca and Calder, 2007). This can be

analyzed by examining the relationship between backscatter values and their Angular Range Analysis (ARA).

**Seabed classification**

Sediment distribution was classified based on backscatter values processed through Angular Range Analysis (ARA) inversion using FMGT software. In this study, 12 sediment classes were identified, namely Muddy Sand, Very Fine Sand, Clayey Sand, Coarse Silt, Sandy Silt, Medium Silt, Sandy Mud, Fine Silt, Sandy Clay, Very Fine Silt, Silty Clay, and Clay, with intensity ranges from ARA as presented in Table 1. The classifications were based on ARA classifications, which were then visualized using ArcGIS software. The visualization effectively showed the distribution of sediment classifications across the study area, as detailed in Figure 3. Based on Table 1, it was found that each sediment class had distinct backscatter intensity and phi ( $\phi$ ) values, reflecting variations in sediment texture and composition. The finer-grained sediment, such as Clay and Silty Clay, represented lower backscatter intensities, signifying softer, more absorbent surfaces.

In contrast, coarser sediments, like Sandy Silt and Very Fine Sand, tended to show higher backscatter intensities due the rougher, harder surfaces, which reflected sound energy more effectively. Based on the sediment classification distribution map, the dominant sediment types in the study area, as signified by their spatial coverage, were coarse silt, sandy silt, and clayey silts. These types are represented by light brown to dark brown shades, as shown in Figure 3. The distribution reflected the prevalence of finer sediment in the study area,

**Table 1.** The intensity and phi range for each seabed sediment class exported from FMGT.

Type	Backscatter (dB)		Phi	
	min	max	min	max
Muddy Sand	-23.91	-21.97	3.06	3.49
Very Fine Sand	-25.81	-22.12	3.5	3.99
Clayey Sand	-27.38	-22.44	4	4.49
Coarse Silt	-29.22	-23.65	4.5	4.99
Sandy Silt	-27.03	-23.67	5	5.38
Medium Silt	-30.91	-25.53	5.52	5.93
Sandy Mud	-29.46	-25.86	6.07	6.49
Fine Silt	-31.30	-26.03	6.63	6.91
Sandy Clay	-29.42	-26.31	7.05	7.47
Very Fine Silt	-31.74	-26.43	7.62	7.9
Silty Clay	-29.59	-26.21	8.04	8.47
Clay	-31.84	-27.16	8.61	9

providing insight into the seabed's sedimentological characteristics and potential depositional environments of seabed. Porosity is a crucial factor in determining backscatter intensity values. Its higher value corresponds to softer, more absorbent sediment types, leading to lower backscatter intensities, as the sound waves were more readily absorbed than reflected (Manik, 2012). In addition to obtaining classification results from MBES data, in-situ sampling was conducted at 15 sample points using a Van Veen grab. Initially, data was proposed to be obtained the data from 100 stations, but due to the time limitation, it was restricted to 15 stations, e.g. 47, 54, 55, 58, 62, 64, 66, 68, 72, 77, 79, 80,

90, 92, and 98 as shown in Table 2. The sample points were determined using a purposive sampling method, about previously acquired backscatter data, and targeted areas with varied seabed sediment types. This method allowed for a comprehensive representation of sediment diversity in the study area, enhancing the accuracy of the sediment classification derived from acoustic data.

Sandy silt sediment was discovered at stations 64, 66, 68, 72, 80, 92, and 98, with an intensity range of 25.93 dB to 26.89 dB. While Clayey sand sediment was observed at stations 55, 62, 79, and 90, within a range of -24.01 dB to -26.97 dB.

**Table 2.** The acoustic sediment classification based on Angular Range Analysis (ARA) at the grab sample positions

Station	East (m)	North (m)	Depth (m)	Back-scatter (dB)	Impedance	Roughness	Phi $\phi$	Sediment Type from grab samples
47	678859.12	9349501.53	-47.61	-27.75	1.20	3.68	4.63	Coarse Silt
54	678651.47	9349202.86	-35.03	-25.78	1.19	3.00	4.79	Coarse Silt
55	678782.24	9349292.40	-45.25	-26.97	1.23	3.68	4.36	Clayey Sand
58	679259.30	9349587.84	-45.13	-28.14	1.19	3.68	4.76	Coarse Silt
62	678428.85	9348810.51	-27.10	-24.01	1.23	2.88	4.36	Clayey Sand
64	678763.82	9348993.89	-30.91	-25.93	1.16	2.75	5.05	Sandy Silt
66	679071.21	9349179.17	-34.79	-26.17	1.15	2.68	5.16	Sandy Silt
68	679385.16	9349382.39	-40.34	-26.89	1.16	2.97	5.06	Sandy Silt
72	678569.13	9348562.00	-32.42	-26.21	1.16	2.73	5.1	Sandy Silt
77	679365.41	9349049.92	-33.50	-26.07	1.21	3.26	4.6	Coarse Silt
79	679644.27	9349310.18	-38.59	-25.63	1.22	3.26	4.45	Clayey Sand
80	678415.92	9348168.71	-32.80	-26.86	1.17	2.98	5.04	Sandy Silt
90	678598.31	9347962.36	-31.69	-25.64	1.22	3.33	4.4	Clayey Sand
92	678871.59	9348133.18	-30.31	-27.30	1.15	2.90	5.2	Sandy Silt
98	679805.00	9348707.29	-28.58	-26.56	1.16	2.89	5.05	Sandy Silt

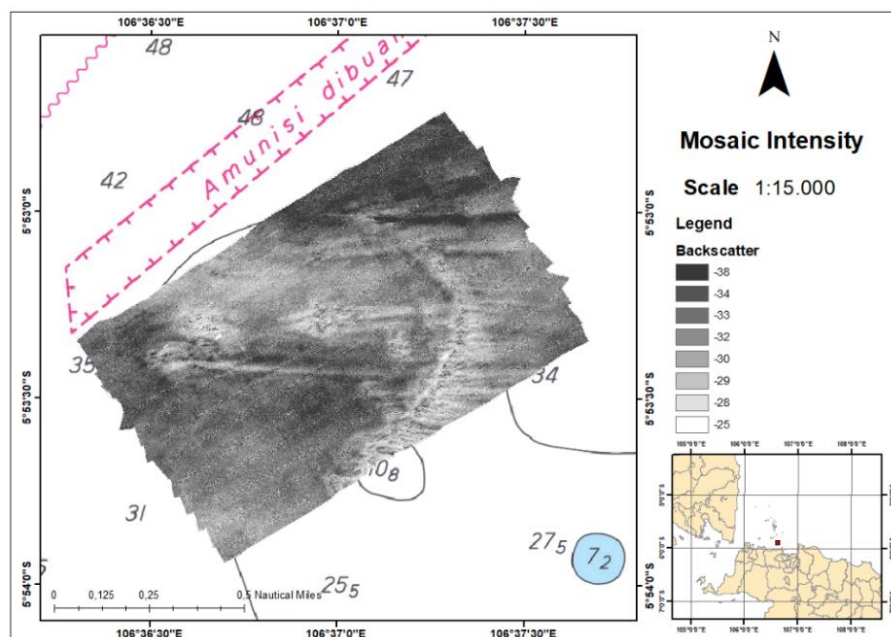


**Figure 2.** Backscatter Mosaic from 400 kHz MBES data at Pari Watters. The color scale of the mosaic intensity from -25 dB to -38 dB

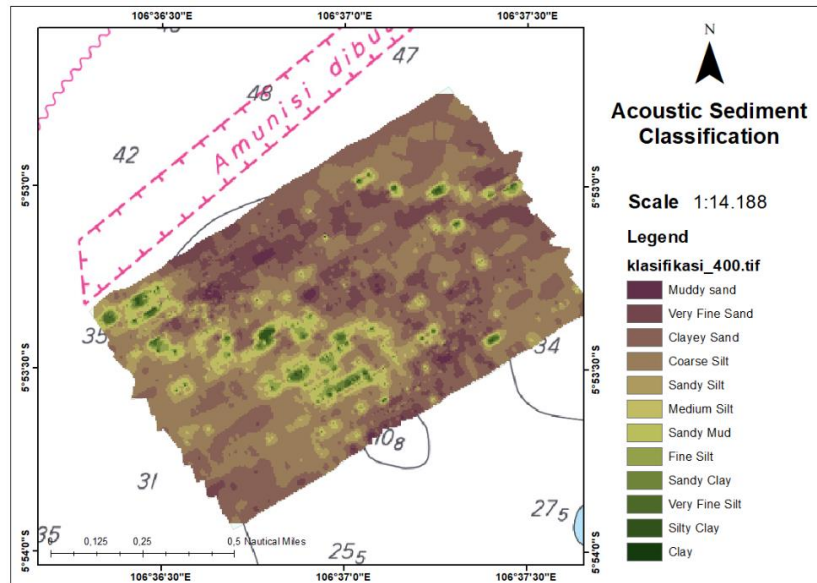


Figure 3. Acoustic Sediment classification using 400 kHz MBES data at Pari Watters

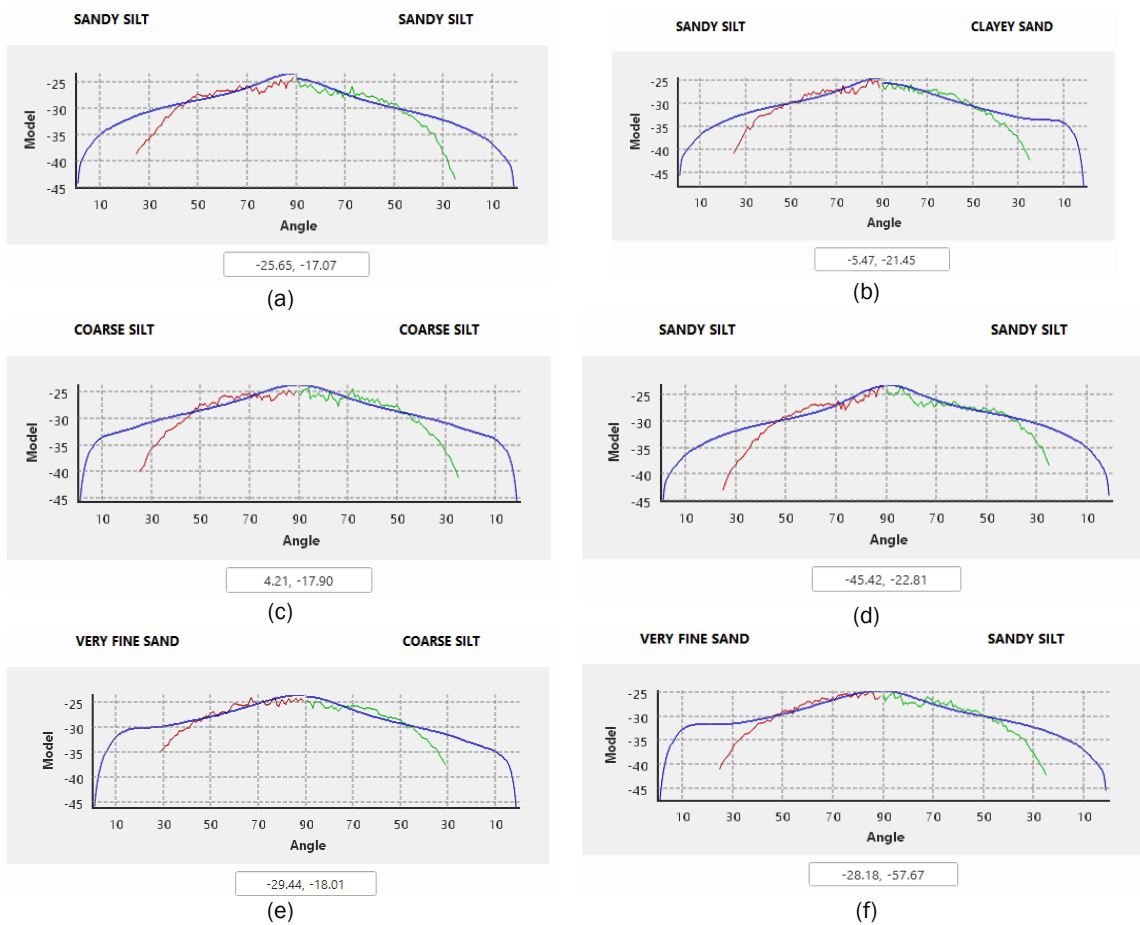


Figure 4. ARA (Angular Range Analysis) curve graph for sediment classification at stations (a) station 98; (b) station 92; (c) station 90; (d) station 62; (e) station 54 dan (f) station 80

Coarse silt sediment are identified at stations 47, 54, 58, and 77. The narrow intensity boundaries between some sediment types led to overlapping intensity values across different sediments. However, this is clarified by the distinction based heavily on phi values or grain size, which aids in accurately differentiating sediment types despite similar intensity ranges.

Sediment sample analysis at various stations is also considered the Angular Range (ARA). Differences between the port and starboard sides of the vessel were observed at the sediment sampling stations, as shown in Figure 4. These differences arise from variations in the angle of incidence, affecting the backscatter response emitted by the sediment, and causing in diverse sediment compositions. As the angle of incidence approaches and diverges from nadir, the backscatter response becomes stronger and weakens, respectively. Additionally, seabed slope and relief impacted the backscatter response, influencing the intensity and

clarity of the received signal (Fonseca *et al.*, 2002). Examples of ARA sampling at stations 98, 97, 90, 62, 54, and 80 for seabed sediment collection are detailed in Figure 4. This featured the methodology and positioning used during sediment sampling, outlining the spatial variability in sediment characteristics as identified through ARA.

The result showed that water depth, seabed relief, and angle orientation substantially impacted sediment classification at a given location, even when the sediment type remained the same. Variations in the incidence angle affected the angular response and acoustic signature of the sediment, leading to potential discrepancies in classification outcomes. As a result, identical sediment types may be classified differently due to variations in the angular response received. This underscores the importance of angle orientation in acoustic-based sediment classification methods (Farihah *et al.*, 2020).

**Table 3.** Sediment Sample Classification Based on the Wentworth Scale (Wentworth, 1922)

Station	Coral >4.75 mm	Gravel > 2 mm	Very Coarse Sand 2-1 mm	Coarse Sand 1-0.5 mm	Medium sand 0.5-0.125 mm	Fine Sand 0.125- 0.063	Clay 0.02 -0.063 mm	Silt <0.063 mm	Sediment Type
47	7.961	5.953	6.903	10.554	11.440	4.334	1.374	1.054	Medium Sand
54	7.748	6.120	3.803	6.323	16.869	7.389	0.849	0.893	Medium Sand
55	3.500	7.895	5.075	5.195	15.395	11.056	1.001	0.550	Medium Sand
58	4.571	9.222	7.194	9.000	12.527	5.019	1.234	0.865	Medium Sand
62	3.053	0.889	5.313	11.560	19.641	8.624	0.562	0.280	Medium Sand
64	0.114	3.300	4.190	9.797	21.033	8.862	1.483	0.882	Medium Sand
66	3.736	4.406	5.491	8.440	17.507	8.099	1.151	0.774	Medium Sand
68	4.578	4.402	12.416	14.757	9.447	2.130	1.105	0.852	Coarse Sand
72	0.271	1.716	5.691	13.180	19.886	7.194	1.339	0.576	Medium Sand
77	13.096	3.798	4.197	10.077	11.830	4.747	1.132	0.741	Coral
79	1.535	5.768	8.288	11.290	15.115	4.958	1.506	1.118	Medium Sand
80	0.064	1.911	4.370	12.248	18.817	9.092	2.106	1.166	Medium Sand
90	0.183	1.448	4.200	11.613	21.016	9.682	1.216	0.584	Medium Sand
92	0.425	2.375	4.494	8.974	19.027	11.575	1.801	0.918	Medium Sand
98	13.007	0.863	4.639	8.906	10.482	6.894	2.898	1.932	Coral

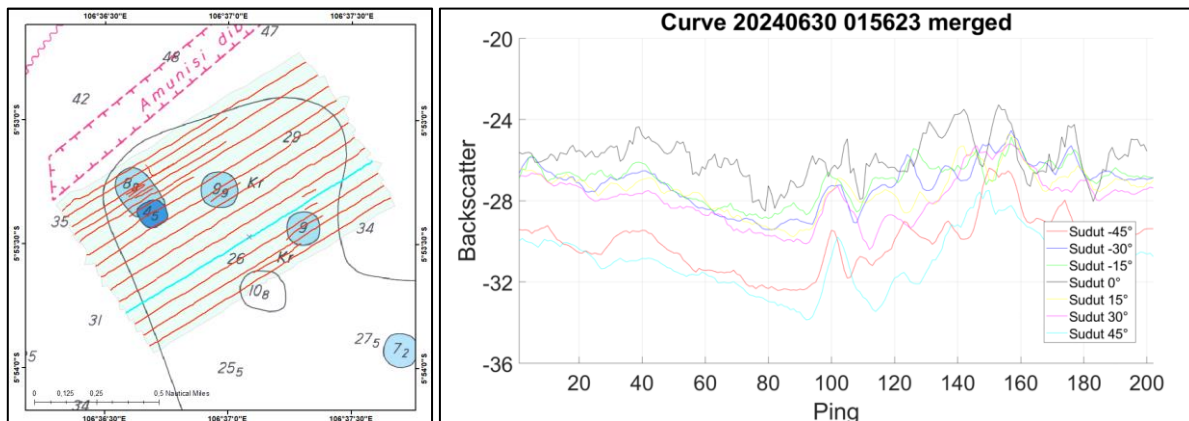


**Figure 5.** ARA (Angular Range Analysis) curve at the blue line incidence angles. -45°, -30°, -15°, 0°, 15°, 30°, 45°

**Table 4.** Comparison between the processing results from FMGT (Fledermaus Geocoder Tools) and in-situ sediment samples

Station	Backscatter (dB)	Wentworth	FMGT
47	-27.75	Medium Sand	Coarse Silt
54	-25.78	Medium Sand	Coarse Silt
55	-26.97	Medium Sand	Clayey Sand
58	-28.14	Medium Sand	Coarse Silt
62	-24.01	Medium Sand	Clayey Sand
64	-25.93	Medium Sand	Sandy Silt
66	-26.17	Medium Sand	Sandy Silt
68	-26.89	Coarse Sand	Sandy Silt
72	-26.21	Medium Sand	Sandy Silt
77	-26.07	Coral	Coarse Silt
79	-25.63	Medium Sand	Clayey Sand
80	-26.86	Medium Sand	Sandy Silt
90	-25.64	Medium Sand	Clayey Sand
92	-27.3	Medium Sand	Sandy Silt
98	-26.56	Coral	Sandy Silt

**Sediment sample analysis**

Sediment samples were processed using a sieve shaker with the dry sieving method, following the Wentworth scale sediment classification. This method include placing dried sediment samples through a series of sieves with progressively smaller mesh sizes. The sieve shaker vibrates the sieves for a set period, allowing particles to be separated by size according to Wentworth's classification categories, such as gravel, very coarse sand, coarse sand, medium sand, fine sand, silt, and clay (Wentworth, 1922). The dry sieving process resulted in the identification of four sediment types based on grain size including Gravel, Coarse Sand, Medium Sand, and Coral.

Sediment size analysis shows that medium sand is the most dominant sediment type at stations 47, 54, 55, 58, 62, 64, 66, 72, 79, 80, 90, and 92. Coarse sand is primarily discovered at station 68, while coral fragments are present at stations 77 and 98. This distribution reflects varying depositional environments, with medium sand mostly showing moderately energetic conditions, coarse sand suggest higher energy, and coral fragments feature biogenic sediment input in specific areas (Manik, 2015; Schimel *et al.*, 2018). Based on Table 4, the comparison between FMGT processing results and in-situ field sample analysis presents significant differences. Sediment classification obtained through FMGT processing suggests a finer seabed sediment texture compared to the in-situ sample results. FMGT results predominantly classify the seabed sediment as sandy silt, followed by coarse silt and clayey sand. In contrast, the in-situ sediment analysis shows that medium sand is the dominant sediment type, accompanied by smaller portions of coarse sand and coral.

This discrepancy may be attributed to the limitations of acoustic data in fully capturing sediment granularity, as FMGT primarily relies on backscatter intensity, which can sometimes overemphasize finer sediment characteristics. In-situ sampling, however, provides direct physical evidence of sediment types, offering a more accurate representation of grain size distributions. The differences underscore the importance of using in-situ sampling to validate acoustic-based classification, specifically when characterizing diverse sediment types on the seafloor.

**Conclusion**

In conclusion, the backscatter intensity mosaic derived from MBES data, with a frequency of 400 kHz, shows a range of -27 dB to -37.5 dB, providing insight into the seabed's texture and composition. High backscatter intensity is correlated with harder and rougher surfaces, while lower intensities are associated with finer, more porous sediment. Variations in the values reflect differences in sediment properties, such as hardness, roughness, and porosity. The application of ARA in FMGT processing showed 12 sediment classes, including sandy silt, coarse silt, and clayey sand, primarily represented in the study area. However, FMGT-based classification tended to favor finer sediment classifications, likely due to acoustic limitations in accurately capturing granular detail. The in-situ analysis, on the other hand, identified medium sand as the dominant sediment type, along with lesser quantities of coarse sand and coral fragments. This suggested that in-situ sampling offered a more direct and precise classification of sediment granularity, particularly for coarser materials. Classification discrepancies observed at the 15 in-situ sampling stations compared to the FMGT processing results



were primarily due to the frequency used in the MBES system. The frequency affected the penetration depth of the acoustic signal, limiting it to the outer surface of the seabed without reaching deeper sediment layers. This limitation was significant because the in-situ data is based on sediment samples acquired with a Van Veen grab, which collected a mixture of surface and subsurface sediment materials, and subsequently analyzed in the laboratory. As a result, the sediment composition identified differed from the FMGT results, which relied solely on the backscatter intensity received from the seabed surface.

## Acknowledgment

The authors would like to express heartfelt gratitude and appreciation to all parties who have contributed to the successful completion of this project. This study was funded by the PDD scheme 2024 and Joint Research Initiative Grant MTCRC 2024.

## References

- Asmoro, N.W., Manik, H.M., Umam, C., Azhari, F., Pranowo, S., Kurniawan, M.A., Setiyadi, J., & Exyas, A. 2024. Analisa Profil Dasar Laut dan Karakteristik Sedimen Menggunakan Multibeam Echosounder di Perairan Jakarta. *J. Geol. Kelaut.*, 22(1): 11–25. <https://doi.org/10.32693/jgk.2.1.1.2024.843>.
- Fahrulian, Manik, H.M., Jaya, I., & Udrek 2016. Angular Range Analysis (ARA) and K-Means Clustering of Multibeam Echosounder Data for Determining Sediment Type. *Ilmu Kelautan: Indonesian Journal of Marine Science*, 21(4): 177–184. <https://doi.org/10.14710/ik.ijms.2.1.4.177-184>.
- Farihah, R.A., Manik, H.M., & Harsono, G. 2020. Pengukuran Dan Analisis Hambur Balik Akustik Menggunakan Teknologi Multibeam Echosounder untuk Klasifikasi Sedimen Dasar Laut Teluk Palu. *J. Ilmu dan Teknol. Kelaut. Trop.*, 12(2): 439–455. <https://doi.org/10.29244/jitkt.v12.i2.28465>.
- Folk, R.L. & Ward, W.C. 1957. Brazos River bar: a study in the significance of grain size parameters. *J. Sediment. Petrol.*, 27(1): 3–26. <https://doi.org/10.1098/rspa.1963.0204>.
- Fonseca, L. & Calder, B. 2005. Geocoder: An Efficient Backscatter Map Constructor. *U.S. Hydro 2005 Conf.*, p. 9.
- Fonseca, L. & Calder, B. 2007. Clustering Acoustic Backscatter in the Angular Response Space. *U.S. Hydro 2007 Conf.*, p. 12.
- Fonseca, L., Mayer, L., Orange, D., & Driscoll, N. 2002. The high-frequency backscattering angular response of gassy sediments: Model/data comparison from the Eel River Margin, California. *J. Acoust. Soc. Am.*, 111(6): 2621–2631. <https://doi.org/10.1121/1.1471911>.
- Fonseca, L. & Mayer, L. 2007. Remote estimation of surficial seafloor properties through the application Angular Range Analysis to multibeam sonar data. *Mar. Geophys. Res.*, 28(2): 119–126. <https://doi.org/10.1007/s11001-007-9019-4>.
- Frederick, C., Villar, S., & Michalopoulou, Z.H. 2020. Seabed classification using physics-based modeling and machine learning. *J. Acoust. Soc. Am.*, 148(2): 859–872. <https://doi.org/10.1121/10.0001728>.
- Innangi, S., Barra, M., Di Martino, G., Parnum, I.M., Tonielli, R., & Mazzola, S. 2015. Reson SeaBat 8125 backscatter data as a tool for seabed characterization (Central Mediterranean, Southern Italy): Results from different processing approaches. *Appl. Acoust.*, 87: 109–122. <https://doi.org/10.1016/j.apacoust.2014.06.014>.
- Jackson, D.R., Winebrenner, D.P., & Ishimaru, A. 1986. Application of the composite roughness model to high-frequency bottom backscattering. *J. Acoust. Soc. Am.*, 79(5): 1410–1422. <https://doi.org/10.1121/1.393669>.
- Janowski, A., Tęgowski, J., & Nowak, J. 2018. Seafloor mapping based on multibeam echosounder bathymetry and backscatter data using Object-Based Image Analysis: A case study from the Rewal site, the Southern Baltic. *Oceanol. Hydrobiol. Stud.*, 47(3): 248–259. <https://doi.org/10.1515/ohs-2018-0024>.
- MacDonald, A. & Collins, C. 2008. Taking Geocoder to Work. *Shallow Surv.* 2008, p. 9.
- Makar, A. 2022. Simplified Method of Determination of the Sound Speed in Water on the Basis of Temperature Measurements and Salinity Prediction for Shallow Water Bathymetry. *Rem. Sens.*, 14(3): p.636. <https://doi.org/10.3390/rs14030636>.
- Manik, H.M. 2012. Seabed identification and characterization using sonar. *Adv. Acoust. Vib.* [Preprint], (February). <https://doi.org/10.1155/2012/532458>.
- Manik, H.M. 2015. Shallow-water acoustics investigations for underwater detection and

- seabed imaging. *Int. J. Appl. Eng. Res.*, 10(17): 38302–38307.
- Manik, H.M., Furusawa, M., & Amakasu, K. 2006. Measurement of sea bottom surface backscattering strength by quantitative echo sounder. *Fish. Sci.*, 72(3): 503–512. <https://doi.org/10.1111/j.1444-2906.2006.01178.x>.
- Manik, H.M., Yulius, D., & Udrekh 2015. Development and application of MB system software for bathymetry and seabed computation. *Int. J. Softw. Eng. its Appl.*, 9(6): 143–160. <https://doi.org/10.14257/ijseia.2015.9.6.15>.
- Medwin, H. 1975. Speed of sound in water: A simple equation for realistic parameters. *J. Acoust. Soc. Am.*, 58: 1318–1319. <https://doi.org/10.1121/1.380790>.
- Medwin, H., Clay, C.S., & Stanton, T.K. 1998. *Fundamentals of Acoustical Oceanography*. *J. Acoust. Soc. Am.* Edited by R. Stern and M. Levy. San Diego, USA: Academic Press. <https://doi.org/10.1121/1.426950>.
- Mustikasari, E. & Rustam, A. 2019. Karakteristik Fisis Air Laut dan Dinamika Perairan Kepulauan Seribu. *J. Ris. Jakarta*, 12(2): 89-98. <https://doi.org/10.37439/jurnaldrd.v12i2.5>.
- Nugroho, C., Manik, H., Gultom, D., & Firdaus, M. 2022. Implementasi Multibeam Echosounder untuk Pengukuran dan Analisis Data Kedalaman Perairan Teluk Jakarta Berdasarkan Standar International Hydrographic Organization, 12(1): p.60. <https://doi.org/10.26418/positron.v12i1.51833>.
- Schimmel, A.C.G., Beaudoin, J., Parnum, I.M., Le Bas, T., Schmidt, V., Keith, G., & Ierodiaconou, D. 2018. Multibeam sonar backscatter data processing. *Mar. Geophys. Res.*, 39(1–2): 121–137. <https://doi.org/10.1007/s11001-018-9341-z>.
- Wendelboe, G. 2018. Backscattering from a sandy seabed measured by a calibrated multibeam echosounder in the 190–400 kHz frequency range. *Mar. Geophys. Res.*, 39(1–2): 105-120. <https://doi.org/10.1007/s11001-018-9350-y>.
- Wentworth, C.K. 1922. A Scale of Grade and Class Terms for Clastic Sediments Author ( s ): Chester K. Wentworth Published by : The University of Chicago Press Stable. *J. Geol.*, 30(5): 377–392.